ACS Catalysis
Research Article
pubs.acs.org/acscatalysis

Hydrogen Transfer versus Methylation: On the Genesis of Aromatics Formation in the Methanol-To-Hydrocarbons Reaction over H-ZSM-5

Juan S. Martínez-Espín,[†,‡] Kristof De Wispelaere,[§] Ton V. W. Janssens,[‡] Stian Svelle,[†] Karl Petter Lillerud,[†] Pablo Beato,[*,‡] Veronique Van Speybroeck,[*,§] and Unni Olsbye[*,†]

[†]Centre for Materials Science and Nanotechnology, Department of Chemistry, University of Oslo, P.O. Box 1033, Blindern, N-0315 Oslo, Norway

[‡]Haldor Topsøe A/S, Haldor Topsøes Allé 1, DK-2800 Kongens Lyngby, Denmark

[§]Center for Molecular Modeling, Ghent University, Technologiepark 903, B-9052 Zwijnaarde, Belgium

Supporting Information

ABSTRACT: The catalytic conversion of methanol (MeOH) and dimethyl ether (DME) into fuels and chemicals over zeolites (MTH process) is industrially emerging as an alternative route to conventional oil-derived processes. After 40 years of research, a detailed mechanistic understanding of the intricate reaction network is still not fully accomplished. The overall reaction is described as two competitive catalytic cycles, dominated by alkenes and arenes, which are methylated and cracked or dealkylated to form effluent products. Herein, we present the reaction of isobutene with methanol and DME as an efficient tool for measuring the relative formation rates of alkenes and arenes, and we provide detailed mechanistic insight into the hydrogen-transfer reaction. We provide experimental and theoretical evidence that manifest a strong competition of methylation and hydrogen transfer of isobutene by methanol, while methylation is substantially favored by DME. Experiments performed at higher conversion facilitate projection of the results to the product distribution obtained when using MeOH or DME as feedstock during the MTH reaction.

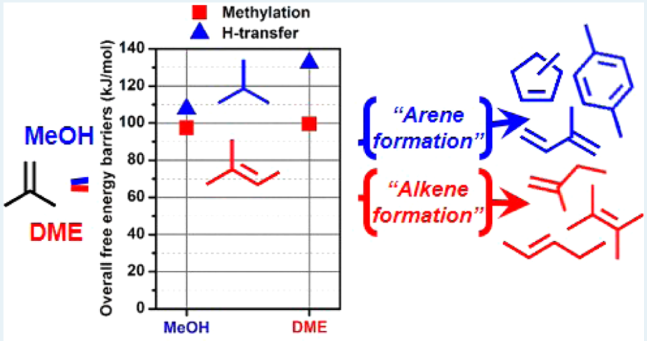

KEYWORDS: *zeolites, methylation, hydrogen transfer, methanol, DME, methanol-to-hydrocarbons*

INTRODUCTION

The quest to disentangle the complex reaction network for the conversion of methanol (MeOH) and dimethyl ether (DME) to hydrocarbons (MTH reaction) over acidic zeolitic materials has motivated an extensive number of publications during the past 40 years.[1−7] It is generally accepted that the hydrocarbon formation is an autocatalytic reaction, where adsorbed hydrocarbon species in the micropores of a zeolitic catalyst, typically alkenes and arenes, also act as "co-catalyst pool species" that boost the conversion of MeOH and DME to hydrocarbons.[8−13] The autocatalytic part of the reaction can be represented by a dual-cycle mechanism, where the two cycles are governed by alkenes and arenes, respectively (Scheme 1).[14]

Each cycle contributes to product formation via sequential methylation and cracking/dealkylation reactions. Methylation entails the incorporation of a methyl group from MeOH or DME into the alkene and arene products, which results in a growth of the hydrocarbon molecules. The rate of methylation reactions depends on factors such as size and branching of the hydrocarbons, the topology and acidity of the zeolitic material used, and the type of methylating agent. Generally, the methylation rate of DME is faster than that of MeOH.[15−22]

Scheme 1. MTH Dual-Cycle Conceptual Mechanism

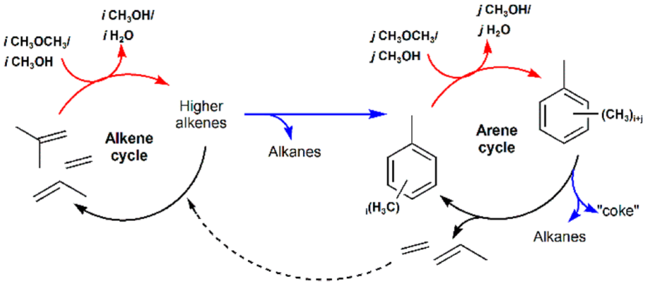

The two cycles are interrelated: dealkylation of polymethylated arenes provides light alkenes to the alkene cycle.[14] Concurrently, cyclization and hydrogen-transfer reactions transform alkenes to arenes and alkanes, thereby promoting the arene cycle (Scheme 1). Further hydrogen transfer from arenes yields polyaromatic molecules and eventually graphitic coke, which contribute to catalyst deactivation (Scheme 1).[23]

Received: May 20, 2017
Revised: July 11, 2017
Published: July 24, 2017

Hydrogen-transfer rates depend on the stability of the intermediate carbenium ions and the strength of the C−H bonds in the hydrogen donor, as well as acidity and topology of the zeolitic catalyst.[22,24,25] Notably, highly substituted alkenes, which may form stable tertiary carbocationic species, i.e., isobutene or triptene, are excellent hydrogen acceptors.[24,25]

Prior studies suggested a direct correlation between arene and alkane selectivity in zeolitic materials, thereby pointing to alkene disproportionation as a hydrogen-transfer pathway.[22,26,27] Recently, however, experiments with feeds of pure alkenes and MeOH−alkene mixtures over H-ZSM-5 catalysts showed that MeOH promotes hydrogen-transfer reactions between alkenes. A formaldehyde intermediate was suggested.[28,29]

Earlier this year, we reported hydrogen-transfer activity when coreacting benzene with MeOH over zeolitic materials. Detailed mechanistic studies showed that a dehydrogenation product, diphenylmethane (DPM), was formed in parallel to the methylation product, toluene. Furthermore, it was shown that the pathway to DPM involves MeOH dehydrogenation. Importantly, DPM was barely observed if benzene was coreacted with DME.[21] DPM and formaldehyde have been classified as coke precursor and coke promoter during hydrocarbon transformations over zeolites.[30−32] Very recently, a strong deactivating role of MeOH compared to DME was demonstrated in the course of the MTH reaction over different zeolite and zeotype catalysts. Furthermore, a significant, but much less pronounced, promotion of arenes and arene-cycle products was observed when the MeOH/DME ratio was increased by changing the feed composition, while the opposite trend was observed by adding MeOH dehydration promoters to the MTH reactor.[33]

The aim of the current contribution is to decipher the reason for the higher selectivity to arenes and arene-cycle products observed when using MeOH compared to DME as MTH feed, as well as to elucidate the mechanism of hydrogen-transfer reactions, i.e., the transformation of alkenes to alkanes and arenes, during MeOH and DME conversion to hydrocarbons.

We selected the cofeeding of isobutene with MeOH and DME over H-ZSM-5 nanosheets at short contact times as a tool to gain fundamental kinetic insight into the overall reaction mechanism. Focus was set on the two reaction classes that determine the relative abundance of alkenes and arenes, as well as the dual-cycle products, i.e., methylation versus hydrogen-transfer reactions; see Scheme 2.

Isobutene was selected as probe molecule because (1) it is an abundant effluent product in the MTH reaction over many catalysts and (2) previous studies suggest that it may adsorb as stable tertiary carbocation under operating conditions, possibly favoring direct hydrogen transfer compared to linear alkenes.[24,25,34−38] Importantly, H-ZSM-5 nanosheets were selected as catalyst for two reasons: (1) H-ZSM-5 is the most industrially relevant MTG catalyst, wherein alkene and arene cycles are clearly observed,[6,14] and (2) the nanosheet morphology enables shortening of the diffusion path of reactants and products,[39] thereby focusing on the kinetic origin of the propagation of alkene- and arene-forming reactions. Further insight into the relative rates of methylation and hydrogen-transfer reactions were provided by isotopic labeling experiments and a set of static and dynamic molecular simulations.

Scheme 2. Visualization of the Competition between Alkene Methylation and Hydrogen Transfer As a Kinetic Tool to Understand Product Selectivity in MTH

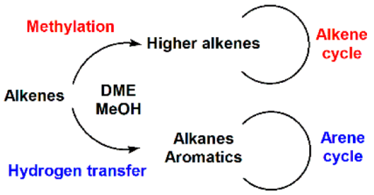

■ EXPERIMENTAL AND THEORETICAL DETAILS

H-ZSM-5 nanosheets were prepared following the protocol described by Choi et al.[40] The sample was also ion-exchanged with Na, leading to a sample with no remaining Brønsted acidity. Details on catalyst characterization can be found in the Supporting Information. Most of the catalytic tests were conducted over H-ZSM-5, and a few tests were conducted over Na-ZSM-5. Typically, 5 mg of catalyst was mixed with 40 mg of quartz, both pressed and sieved to 250−420 μm particle size, to ensure isothermal conditions and limit conversion level. The tests were carried out in a 6 mm internal diameter quartz U-shaped reactor. A thermocouple inserted in a 3 mm wide quartz sleeve in contact with the catalyst bed monitored reaction temperature. ^{12}C-MeOH (VWR, 99.8%), ^{13}C-MeOH (Cambridge Isotope Laboratories, 99%), dimethyl ether (AGA, 25 mol % DME/Argon 6.0), and isobutene (AGA, 99.9%) were used as reactants. Liquid reactants were fed by flowing a helium stream through a flask of boiling reactant, and the saturated stream was passed through a water-cooled Vigreux condenser kept at 35 °C. A third feed line with helium was used to adjust the desired contact times. Catalyst activation and regeneration were carried out by initially heating with a 5 °C/min ramp under 20% O_2 in helium to 550 °C, and then temperature was kept for 1 h under 100% O_2. Subsequently, the catalyst was cooled to reaction temperature under a helium stream. Isobutene (40 mbar) was reacted alone or coreacted with equimolar amounts of oxygenates (MeOH and/or DME) at 350 °C, 1 bar, and total flow equal to 100 mL/min. Contact time variation tests were conducted by adjusting the total flows at constant temperature and partial pressures, changing space velocity from 3 to 12 g_{cat}·min/mL. The effluent of the reactor was analyzed by GC/MS (Agilent 7890) with flame ionization detector and 5975C MS detector using two Restek Rtx-DHA-150 columns.

Density functional theory (DFT) calculations were carried out with the Vienna Ab Initio Simulation Package (VASP 5.3) using the PBE-D3 functional to account for the dispersion interactions.[41−45] The projector augmented wave (PAW) method was used, a plane-wave cutoff of 600 eV was adopted, and the self-consistent field (SCF) convergence criterion was set to 10^{-5} eV. The Brioullin zone sampling was restricted to the Γ-point. Transition states were initially optimized with the improved dimer method and then refined with a quasi-Newton algorithm. Geometries were slightly displaced along the normal mode corresponding to the motion that leads the system over the barrier to generate starting geometries for the optimization of reactant and product states. For these calculations a conjugate gradient algorithm was applied. A periodic H-ZSM-5 model was used, consisting of 96 T atoms and one substitutional Al defect at the T12 position, similar to that in earlier work.[21,46,47] The unit cell parameters were defined via a Birch−Murnaghan equation of state fit and set to a = 20.02 Å, b

= 20.25 Å, c = 13.49 Å, α = 89.87°, β = 89.69°, and γ = 90.10°. For the normal-mode analysis (NMA), a partial Hessian vibrational analysis (PHVA) was performed using VASP and our in-house toolkit TAMkin.[48] The guest molecules and an 8T framework cluster were taken into account during the NMA. As the potential energy surface (PES) is relatively flat, it can be hard to remove all imaginary frequencies, as was also pointed out by De Moor et al.[49] Spurious imaginary frequencies were substituted by an arbitrary value of 50 cm^{-1}, as done in earlier work.[21] A similar procedure with a value of 12 cm^{-1}, as done by Brogaard et al.,[50] led to slightly different free energy values but did not alter the conclusions from the computational study (shown in the Supporting Information). Apart from the static calculations, a series of ab initio molecular dynamics simulations were performed to follow some products dynamically. Ten ps molecular dynamics (MD) simulations were performed in periodic H-ZSM-5 models with the CP2K simulation package (version 2.7),[51,52] using the revPBE-D3 level of theory, a DZVP-GTH basis set, and pseudopotentials.[53] The simulations were performed in the NPT ensemble at 250 °C and around 1 bar. The temperature and pressure were controlled via a chain of 5 Nosé−Hoover thermostats and an MTK barostat, respectively.[54,55] An integration time step of 0.5 fs was applied.

RESULTS AND DISCUSSION

Experimental Assessment of the Reactivity of Isobutene Alone and in the Presence of MeOH and DME. First, we compare the reactivity of isobutene alone and coreacted with MeOH and DME to identify the impact of the oxygenates compared to pure isobutene reactions (Figure 1). The colored scheme in Figure 2 (bottom) aims to guide the reader to describe the dominant reaction pathways for all effluent products observed from the isobutene reactions in the absence and presence of MeOH and DME. In agreement with recent literature, MeOH/isobutene feed promotes the formation of alkanes (predominantly isobutane) and polyunsaturated hydrocarbons (vide infra), compared to pure isobutene feed.[28,29] In spite of the higher total conversion rate of the DME/isobutene feed, a lower net formation rate toward alkanes and polyunsaturated hydrocarbons is observed, relative to the MeOH/isobutene feed (Figure 1). These results confirm the important role of MeOH as a promoter of hydrogen-transfer reactions, which lead to alkanes and polyunsaturated hydrocarbons. Furthermore, they show that DME also promotes hydrogen-transfer reactions, but to a much lesser degree than MeOH. Interestingly, a reduction in the formation rate of C_4 isomers in the presence of MeOH and DME is observed, relative to the pure isobutene feed. Under the low conversion levels achieved (<18%), it is expected that isomerization is the main reaction involved in C_4 isomers formation from isobutene. As earlier reported by Svelle et al.,[17] the presence of MeOH and DME suppresses alkene isomerization, in favor of competing reactions.

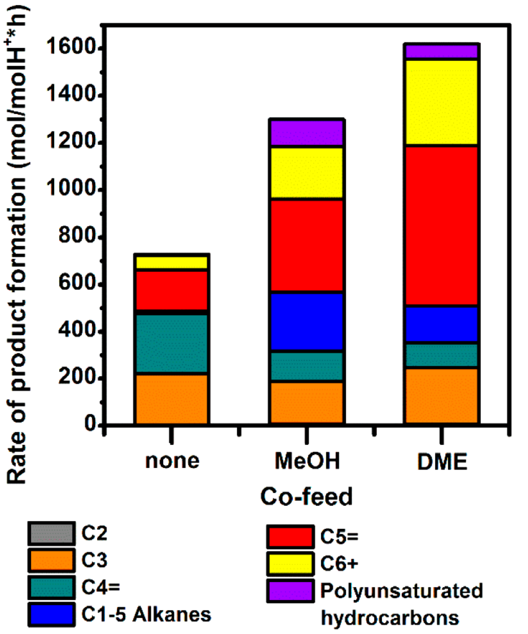

Figure 1. Net product formation rates from isobutene (40 mbar) reacted alone and coreacted with MeOH (40 mbar) and DME (40 mbar) over H-ZSM-5 at 350 °C. Total conversion = 9.5−17.4%.

To further investigate the effect of each oxygenate, we carefully coreacted equimolar isobutene and MeOH/DME mixtures, a strategy that yielded key information on the net formation rates and mechanisms of primary and secondary products. The results are presented in Figure 2 (top panel).

Focusing first on the primary products observed (Figure 2, top left panel), larger fractions of DME in the feed promote the formation of 2-methyl-2-butene (2M2B), which is the direct methylation product from isobutene. In contrast, increasing the fraction of MeOH in the oxygenate cofeed, despite the lower overall activity, leads to a steady promotion of the formation rate of isobutane, which is the direct hydrogen-transfer product from isobutene. These results, combined with the nearly null isobutane formation from pure isobutene feed, suggest that MeOH is involved in a bimolecular hydrogen-transfer reaction from isobutene to isobutane. However, as implied also from the results in Figure 1, the hydrogen-transfer activity is significant also in the presence of DME. Importantly, the inverse trends observed for the formation rates of the methylation product, 2M2B, and the hydrogenation product, isobutane, suggest that they are formed by parallel, possibly competitive reactions (Figure 2, top left panel). The last product family in the top left panel of Figure 2 shows that the formation rate of linear C_4 isomers from isobutene is suppressed to a similar extent by MeOH and DME (see also Figure 1).

Secondary products are plotted in the top middle and top right panels of Figure 2. They are grouped according to their formation rate trend with increasing MeOH fractions in the oxygenate feed: the products in the top middle panel are promoted by DME, while most of the products in the top right panel are promoted by MeOH. As a guide to the reader, the color code of the experimental data in the top panels corresponds to that of the reaction classes to which they are allocated, shown in the bottom panel of Figure 2.

The C_{6+} monoalkene hydrocarbons are grouped together (Figure 2, top middle panel). These products may result from C_5 sequential methylation and possible dimerization/(cracking) reactions. The extent of dimerization/(cracking) might be determined from experiments with pure isobutene feeds, as this reaction occurs in the absence of MeOH/DME (Figure 1). Clearly, the formation rates of C_{6+} monoalkene hydrocarbons are much faster with MeOH/DME presence. Therefore, these results suggest that most C_{6+} hydrocarbons are formed via sequential methylation. Importantly, these products are formed faster with DME compared to MeOH. The same trend is

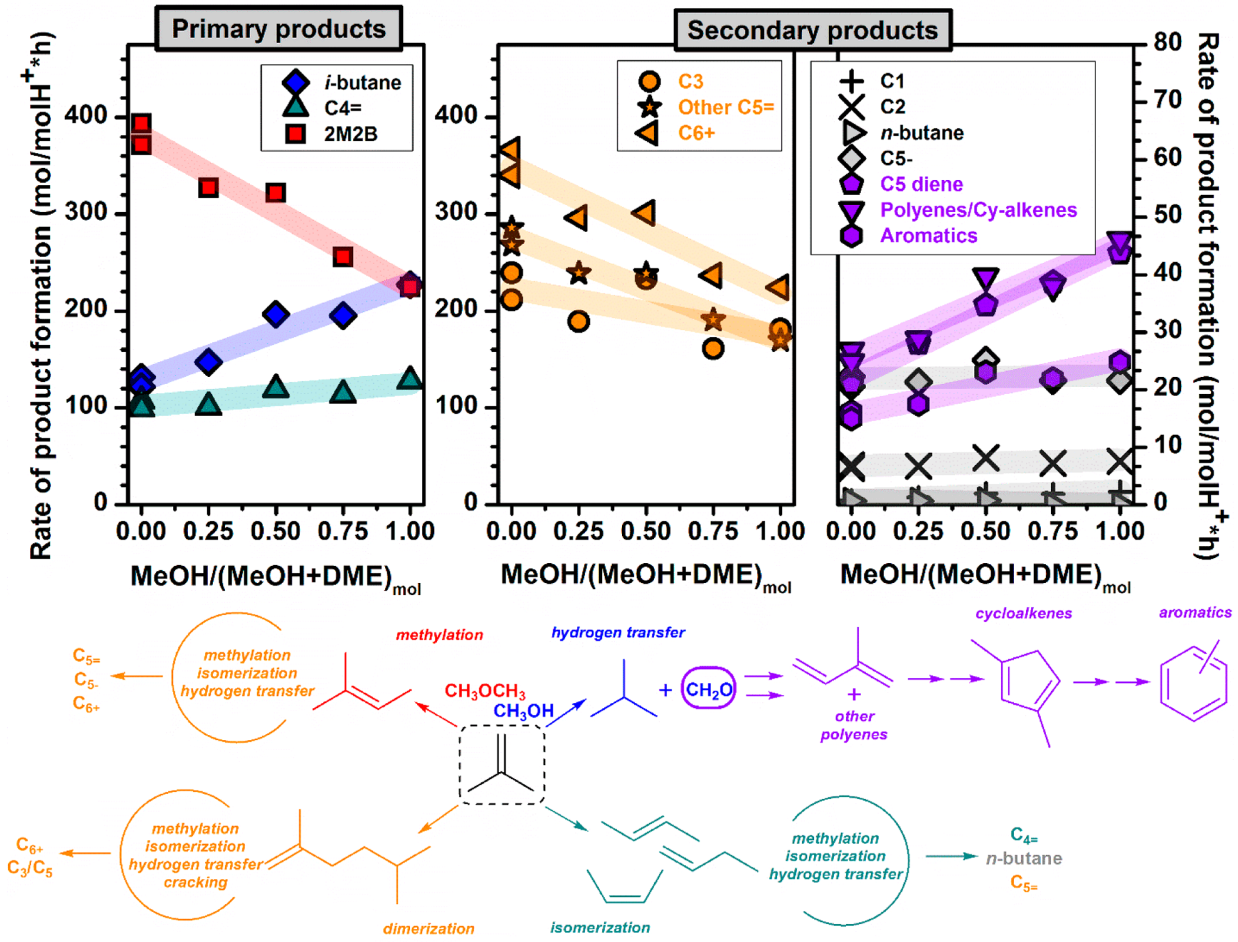

Figure 2. (Top) Net product formation rates during coreactions of isobutene (40 mbar) with different MeOH/DME mixtures (40 mbar) over H-ZSM-5 at 350 °C. Total conversion = 12.7−17.8%. (Bottom) Proposed predominant reaction pathways during coreaction of isobutene with MeOH/DME. The color scheme is the same in the top and bottom panels and aims to serve as a guide to correlate the origin of all products observed and their formation rates.

observed in the formation rates of C_5 alkene isomers, which exclude the primary methylation product (2M2B). These products may derive from methylation/isomerization and/or dimerization/cracking reactions. As observed for C_{6+} hydrocarbons, C_5 alkene isomers are promoted by DME compared to MeOH and are substantially suppressed in the absence of DME and MeOH (Figure 1). The last product group that is promoted by DME corresponds to C_3, nearly exclusively propene. This short product might be formed either directly from DME, from cracking of higher alkenes, or from aromatics dealkylation.[14,56,57] The low conversion levels and small amount of aromatics produced suggest a negligible contribution of dealkylation reactions to C_3 fraction. Thus, its formation from hydrogen-transfer-derived products (aromatics) can be ruled out. The most probable routes are then alkene cracking or direct DME conversion.

MeOH, in addition to the hydrogen-rich product (isobutane, top left panel), promotes a series of hydrogen-deficient products to satisfy stoichiometric demands (top right panel): C_5 diene (isoprene), polyenes−cycloalkenes, and aromatics (see mass balance and chromatograms in Supporting Information), as highlighted by the blue pathway in Figure 2 (bottom panel). Hence, a solid link between MeOH and products derived from hydrogen-transfer reactions (isobutane, isoprene, polyenes, cycloalkenes, and arenes) is established. In summary, these experiments show that MeOH enhances hydrogen-transfer reactions in its interaction with isobutene compared to DME.

Importantly, the most abundant diene observed is isoprene (top right panel), while no butadiene is detected. This observation suggests that diene formation is preceded by an addition reaction, instead of alkene dehydrogenation. Furthermore, the opposite trends observed in the formation rates of 2M2B and isoprene with increasing MeOH fractions (top left panel) suggest that 2M2B is not an intermediate in isoprene formation. On the basis of recent studies proposing the presence of formaldehyde under MTH-related conditions,[21,28,31,58,59] as well as the well-documented synthesis of isoprene and other polyenes from alkenes and aldehydes (Prins reaction),[60−62] we hypothesize that MeOH (and to a lesser extent DME) induces hydrogen-transfer reactions leading to alkanes and formaldehyde. Formaldehyde may react with isobutene and other alkenes in the hydrocarbon-pool to give isoprene and polyene hydrocarbons, respectively. Subsequently, these polyenes can act as intermediates in the formation of aromatic molecules (Figure 2, top right panel), as indicated previously by the groups of Haw and Hunger and reflected in Figure 2 (bottom).[63,64] Therefore, a distinctive kinetic role of

DOI: 10.1021/acscatal.7b01643
ACS Catal. 2017, 7, 5773−5780

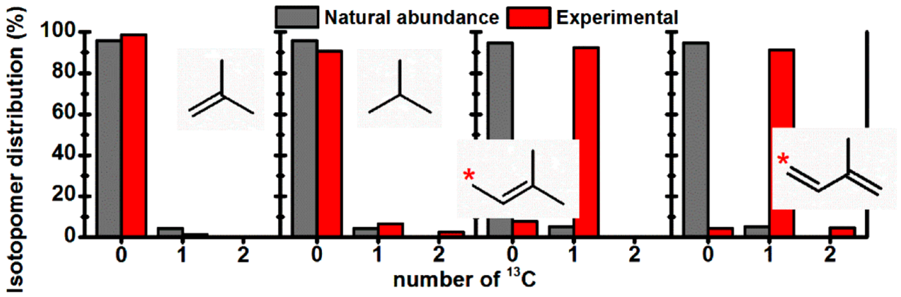

Figure 3. Isotopomer distribution of isobutene, isobutane, 2-methyl-2-butene, and isoprene during coreactions of isobutene (40 mbar) with ^{13}C-MeOH (40 mbar) over H-ZSM-5 at 350 °C. Flow = 100 mL/min. Total conversion = 17.8%.

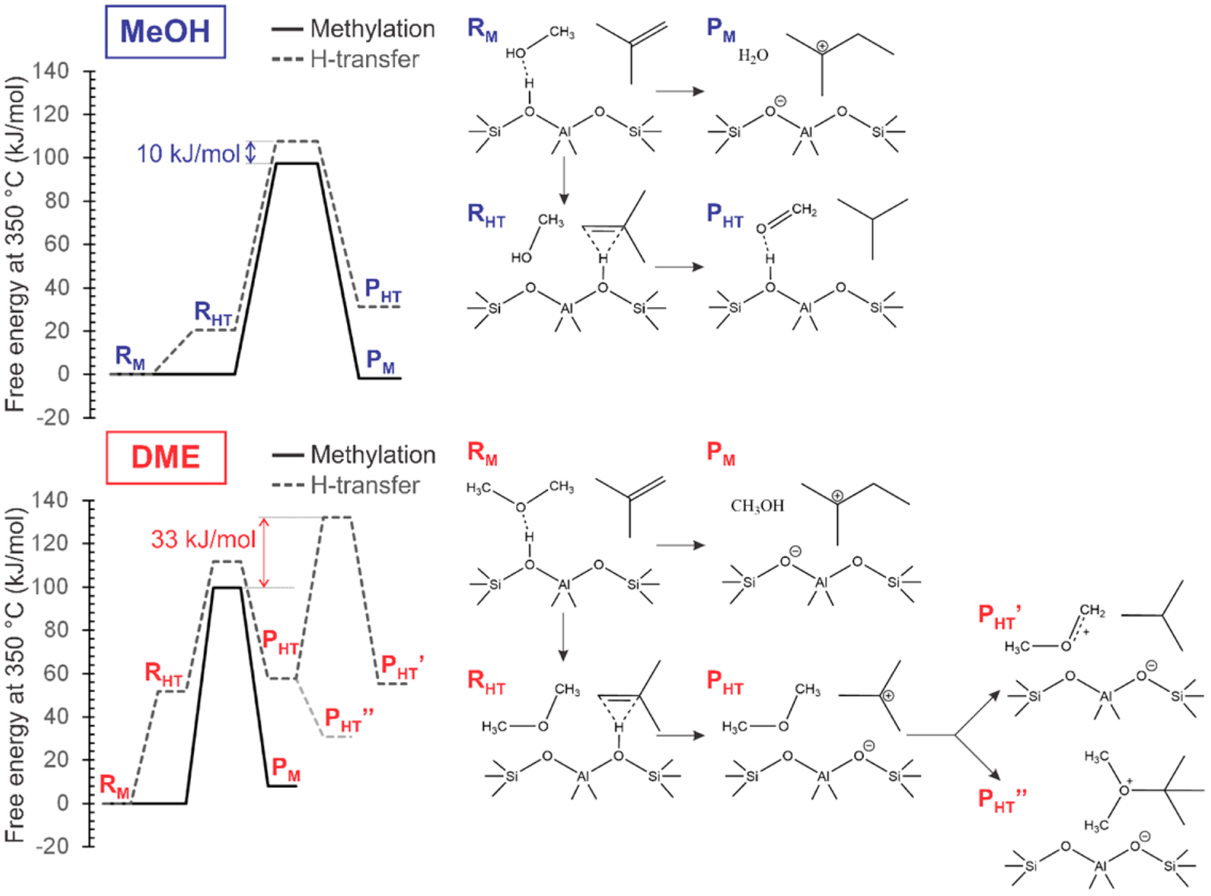

Figure 4. Free energy profile of isobutene methylation and hydrogen-transfer reactions with MeOH (top) and DME (bottom). The right panels show the mechanism and stable states as indicated in the free energy profiles.

MeOH and DME in their interaction with isobutene is observed. This difference entails a different steady-state concentration of alkenes and arenes in the zeolite pores during the MTH reaction, which is key to understanding the higher selectivity toward arenes and arene-cycle products when using MeOH compared to DME as MTH feedstock over the H-ZSM-5 catalyst.

To further investigate the formation mechanism of the most relevant products, labeled ^{13}C-MeOH was coreacted with isobutene. The experiments show that isobutene in the effluent does not contain labeled carbon (Figure 3). This means that the conversion level is sufficiently low as to not produce substantial amounts of isobutene via secondary reactions, thereby facilitating the mechanistic interpretation of the data. With regards to the main hydrogen-transfer product, non-labeled isobutane dominates the isotopomer distribution and thus corroborates its direct formation from isobutene. Interestingly, the main methylation product, 2M2B, shows the incorporation of 1 labeled carbon from MeOH. This confirms that direct methylation of isobutene is the main pathway involved in its formation, and other pathways, i.e., dimerization/cracking, are not significant under the conditions tested. In the same way, monolabeled isoprene dominates the isotopomer distribution, proving the direct incorporation of MeOH carbon into the diene product. These results are also consistent with the hypothesis involving an already-oxidized derivative from MeOH (formaldehyde) and isobutene in the formation of isoprene.

Recently, a possible contribution of Lewis acid sites in hydrogen-transfer reactions during the MTH reaction was

DOI: 10.1021/acscatal.7b01643
ACS Catal. 2017, 7, 5773−5780

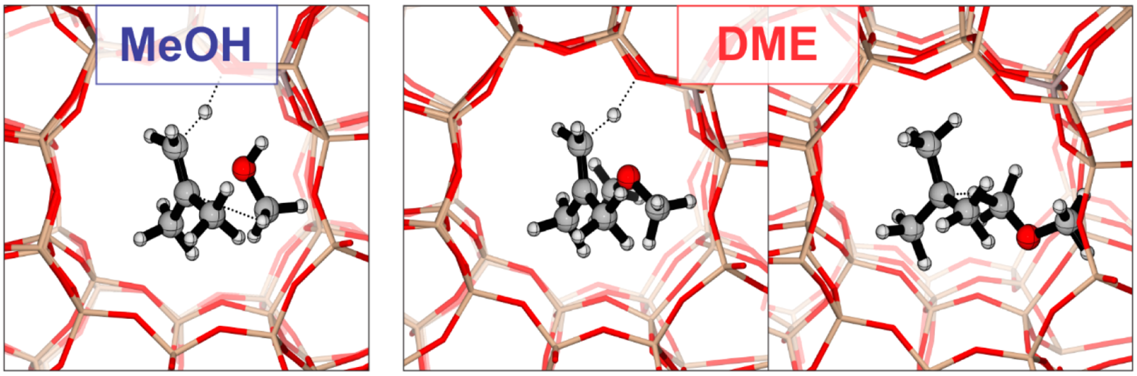

Figure 5. Visualization of the hydrogen-transfer transition states between isobutene and MeOH (left) or DME (right) in H-ZSM-5. For MeOH a concerted pathway was found, whereas for DME only a stepwise pathway could be located.

hypothesized.[28] To elucidate the nature of the reaction centers during isobutene cofeed with MeOH/DME, H-ZSM-5 was ion-exchanged with Na. Consequently, Na-ZSM-5 presents only Lewis acidity corresponding to Na and extraframework aluminum. The catalytic results (shown in the Supporting Information) reveal negligible activity of this sample, meaning that isolated Lewis sites do not contribute to the results presented in Figure 2.

Theoretical Assessment of the Competitive Isobutene Methylation and Hydrogen Transfer with MeOH and DME. Our experimental observations were complemented by a set of density function theory (DFT) calculations to rationalize the substantially different selectivity toward hydrogen-transfer products in the experiments with MeOH and DME. Figure 4 displays the free energy profiles at 350 °C for isobutene methylation and isobutane formation with MeOH (top panel) and DME (bottom panel) on a Brønsted acid site (BAS) in H-ZSM-5 obtained after static DFT calculations. All free energy profiles are expressed with respect to MeOH adsorbed on the BAS and coadsorbed isobutene such that intrinsic methylation barriers are reported.[65,66] A hydrogen-transfer mechanism could be identified starting from an isobutene π-complex and leading to the formation of isobutane and formaldehyde in the case of MeOH (product $\mathbf{P}_{\mathbf{HT}}$) or a methoxymethyl cation in the case of DME (product $\mathbf{P}_{\mathbf{HT}}'$). During the hydrogen-transfer reaction, isobutene gets protonated by the BAS and a hydride shift takes place between the methyl group of the oxygenate and the *t*-butyl cation. These two steps were found to occur simultaneously with MeOH, whereas for DME a two-step process was found (Figure 5). Note that the intermediate formation of a *t*-butyl carbocation stabilizes the transition state and intermediate $\mathbf{P}_{\mathbf{HT}}$ in the MeOH and DME pathways, respectively. The methylation was modeled as a concerted reaction step, as at the applied conditions this reaction was earlier found to be the dominant methylation mechanism.[20,67]

The differences between the overall free energy barriers for the methylation and hydrogen-transfer reactions were found to be 10 kJ/mol for MeOH and 33 kJ/mol for DME. Note that the less-efficient adsorption of isobutene compared to the oxygenates on the BAS (states $\mathbf{R}_{\mathbf{M}}$ vs $\mathbf{R}_{\mathbf{HT}}$) contribute to the overall hydrogen-transfer barrier. While the methylation and hydrogen-transfer reactions are clearly in competition with MeOH as reactant, the relative rate of hydrogen transfer with DME is predicted to be lower, which correlates well with the experimental findings. Furthermore, short ab initio molecular dynamics (MD) simulations revealed the existence of an additional stable state formed by DME and a *t*-butyl cation $\mathbf{P}_{\mathbf{HT}}''$ (see Supporting Information). The stepwise nature of the hydrogen-transfer reactions allows the formation of a relatively stable *t*-butyl dimethyl oxonium ion. This type of molecule is often related to direct C−C bond formation during the MTH reaction.[27,68,69] Therefore, our theoretical study confirms that hydrogen-transfer reactions are in strong competition with methylation reactions when cofeeding MeOH and isobutene. When DME is fed instead, the higher overall barrier, more complex process, and competition with the formation of a stable cation make hydrogen transfer less efficient.

Impact of Competing Methylation and Hydrogen Transfer in the MTH Reaction. We further evaluated the interplay of isobutene with MeOH and DME during experiments conducted at higher conversion levels (15−45%) to assess whether the kinetic and mechanistic differences observed at lower conversion are also reflected in a larger hydrocarbon pool, more similar to the one present during the MTH reaction. With increasing contact time, all product yields increase, except the isoprene yield (Figure 6), thereby implying its intermediate role in the formation of polyunsaturated hydrocarbons, such as aromatics, as illustrated in Figure 2 (bottom). Furthermore, the yields of alkenes, alkanes, and polyunsaturated hydrocarbons

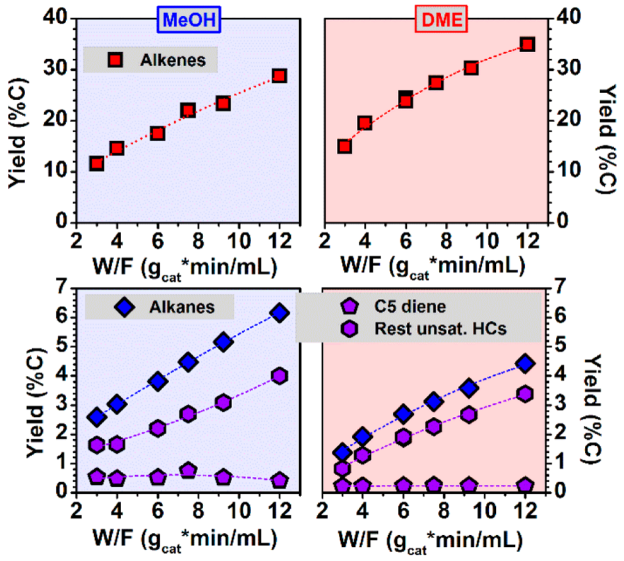

Figure 6. Yield of products (% C) during coreactions of isobutene (40 mbar) with MeOH (40 mbar) and DME (40 mbar) over H-ZSM-5 at 350 °C. Total conversion = 16.4−43.0%.

remain markedly different for MeOH and DME cofeeds under these broad conversion levels. As also observed at lower conversion, hydrogen-transfer products are produced to a larger extent in the presence of MeOH. This result validates the use of isobutene coreaction with MeOH and DME to measure the nature of hydrocarbon pool species operating in the MTH reaction, helping to explain the effluent product distribution of this complex reaction.

The different rates of MeOH and DME toward isobutene methylation and hydrogen-transfer reactions observed in this work are in full agreement with, and serve to explain, the differences in effluent selectivity that were observed when feeding either MeOH or DME over a H-ZSM-5 catalyst under MTH conditions.[33] The results imply that the ratio of MeOH/DME in the reactor under MTH operation will affect the relative extent of the alkene and arene cycles. As MeOH promotes hydrogen transfer compared to DME, it promotes the formation of alkanes, aromatics, and coke (Scheme 1).

■ CONCLUSION

This work presents the coreaction of isobutene with MeOH and DME as a tool to comprehend the origin of the aromatic hydrocarbons involved in the important autocatalytic stage of the MTH reaction. The relative rates of methylation and hydrogen-transfer reactions influence the steady-state concentration of alkenes and arenes in the zeolitic pores and, hence, the relationship between the catalytic alkene and arene cycles. Consequently, this contribution gives an insightful perspective of the MTH product distribution.

The application of experimental and theoretical methods of the coreaction of isobutene with MeOH and DME over H-ZSM-5 reveals different abilities of the two oxygenates toward methylation and hydrogen-transfer reactions. While methylation rates of DME are considerably faster than its hydrogen-transfer activity, MeOH rates for both reactions are equally competitive under the conditions used in this work. Furthermore, formation of secondary products clearly differs according to the oxygenate cofed with isobutene. Formaldehyde is proposed as oxidized hydrogen-transfer product from MeOH, while alkanes are the reduced products. The presence of formaldehyde also induces the formation of hydrogen-deficient hydrocarbons, with aromatics, and possibly coke, being the end-products. This means that promoting isobutene hydrogen transfer with respect to methylation is equivalent to promoting the arene cycle in the MTH reaction. In this work, we provide a solid base to rationalize the effect of MeOH/DME ratio on the product distribution of the MTH reaction, linking MeOH to the promotion of the arene cycle in MTH as highlighted in Scheme 1.

■ ASSOCIATED CONTENT

Supporting Information

The Supporting Information is available free of charge on the ACS Publications website at DOI: 10.1021/acscatal.7b01643.

> Detailed information about material synthesis, acid site measurements, cofeed product composition, influence of Lewis acid sites, DFT modeling, and MD simulations (PDF)

■ AUTHOR INFORMATION

Corresponding Authors

*E-mail: pabb@topsoe.com.
*E-mail: veronique.vanspeybroeck@ugent.be.
*E-mail: unni.olsbye@kjemi.uio.no.

ORCID

Unni Olsbye: 0000-0003-3693-2857

Notes

The authors declare no competing financial interest.

■ ACKNOWLEDGMENTS

J.S.M.-E., T.V.W.J., S.S., K.P.L., P.B., and U.O. acknowledge the financial support received via the European Industrial Doctorates project "ZeoMorph" (FP7 ITN-EID), part of the Marie Curie actions (Grant agreement no. 606965). Dr Bjørn Tore Lønstad Bleken is acknowledged for the synthesis of the H-ZSM-5 sample. K.D.W. and V.V.S. acknowledge the Fund for Scientific Research—Flanders (FWO), the Belgian American Educational Foundation, the Research Board of Ghent University (BOF), BELSPO, in the frame of IAP/7/05 funding from the European Union's Horizon 2020 research and innovation program (consolidator ERC Grant agreement no. 647755—DYNPOR (2015—2020)). The computational resources and services used were provided by Ghent University (Stevin Supercomputer Infrastructure) and the VSC (Flemish Supercomputer Center), funded by the Research Foundation—Flanders (FWO).

■ REFERENCES

(1) Chang, C. D.; Silvestri, A. J. *J. Catal.* **1977**, *47*, 249−259.
(2) Hutchings, G. J.; Hunter, R. *Catal. Today* **1990**, *6*, 279−306.
(3) Stöcker, M. *Microporous Mesoporous Mater.* **1999**, *29*, 3−48.
(4) Keil, F. J. *Microporous Mesoporous Mater.* **1999**, *29*, 49−66.
(5) Haw, J. F.; Song, W.; Marcus, D. M.; Nicholas, J. B. *Acc. Chem. Res.* **2003**, *36*, 317−326.
(6) Olsbye, U.; Svelle, S.; Bjørgen, M.; Beato, P.; Janssens, T. V. W.; Joensen, F.; Bordiga, S.; Lillerud, K. P. *Angew. Chem., Int. Ed.* **2012**, *51*, 5810−5831.
(7) Hemelsoet, K.; Van Der Mynsbrugge, J.; De Wispelaere, K.; Waroquier, M.; Van Speybroeck, V. *ChemPhysChem* **2013**, *14*, 1526−1545.
(8) Chen, N. Y.; Reagan, W. J. *J. Catal.* **1979**, *59*, 123−129.
(9) Song, W.; Marcus, D. M.; Fu, H.; Ehresmann, J. O.; Haw, J. F. *J. Am. Chem. Soc.* **2002**, *124*, 3844−3845.
(10) Dahl, I. M.; Kolboe, S. *J. Catal.* **1996**, *161*, 304−309.
(11) Dahl, I. M.; Kolboe, S. *J. Catal.* **1994**, *149*, 458−464.
(12) Xu, T.; White, J. L. Catalyst pretreatment in an oxygenate to olefins reaction system. U.S. Patent 6,734,330, May 11, 2004.
(13) Xu, T.; White, J. L. Catalyst pretreatment in an oxygenate to olefins reaction system. U.S. Patent 6,743,747, June 1, 2004.
(14) Bjørgen, M.; Svelle, S.; Joensen, F.; Nerlov, J.; Kolboe, S.; Bonino, F.; Palumbo, L.; Bordiga, S.; Olsbye, U. *J. Catal.* **2007**, *249*, 195−207.
(15) Hill, I. M.; Ng, Y. S.; Bhan, A. *ACS Catal.* **2012**, *2*, 1742−1748.
(16) Svelle, S.; Kolboe, S.; Swang, O.; Olsbye, U. *J. Phys. Chem. B* **2005**, *109*, 12874−12878.
(17) Svelle, S.; Rønning, P. O.; Olsbye, U.; Kolboe, S. *J. Catal.* **2005**, *234*, 385−400.
(18) Svelle, S.; Rønning, P. O.; Kolboe, S. *J. Catal.* **2004**, *224*, 115−123.
(19) Van der Mynsbrugge, J.; De Ridder, J.; Hemelsoet, K.; Waroquier, M.; Van Speybroeck, V. *Chem. - Eur. J.* **2013**, *19*, 11568−11576.
(20) Westgård Erichsen, M.; De Wispelaere, K.; Hemelsoet, K.; Moors, S. L. C.; Deconinck, T.; Waroquier, M.; Svelle, S.; Van Speybroeck, V.; Olsbye, U. *J. Catal.* **2015**, *328*, 186−196.
(21) Martinez-Espin, J. S.; De Wispelaere, K.; Westgård Erichsen, M.; Svelle, S.; Janssens, T. V. W.; Van Speybroeck, V.; Beato, P.; Olsbye, U. *J. Catal.* **2017**, *349*, 136−148.

(22) Ilias, S.; Bhan, A. *ACS Catal.* **2013**, *3*, 18−31.
(23) Olsbye, U.; Svelle, S.; Lillerud, K. P.; Wei, Z. H.; Chen, Y. Y.; Li, J. F.; Wang, J. G.; Fan, W. B. *Chem. Soc. Rev.* **2015**, *44*, 7155−7176.
(24) Simonetti, D. A.; Carr, R. T.; Iglesia, E. *J. Catal.* **2012**, *285*, 19−30.
(25) Simonetti, D. A.; Ahn, J. H.; Iglesia, E. *J. Catal.* **2011**, *277*, 173−195.
(26) Ilias, S.; Bhan, A. *J. Catal.* **2012**, *290*, 186−192.
(27) Stöcker, M. *Microporous Mesoporous Mater.* **1999**, *29*, 3−48.
(28) Müller, S.; Liu, Y.; Kirchberger, F. M.; Tonigold, M.; Sanchez-Sanchez, M.; Lercher, J. A. *J. Am. Chem. Soc.* **2016**, *138*, 15994−16003.
(29) Sun, X.; Müller, S.; Liu, Y.; Shi, H.; Haller, G. L.; Sanchez-Sanchez, M.; Van Veen, A. C.; Lercher, J. A. *J. Catal.* **2014**, *317*, 185−197.
(30) Guisnet, M.; Magnoux, P. *Appl. Catal., A* **2001**, *212*, 83−96.
(31) Hwang, A.; Kumar, M.; Rimer, J. D.; Bhan, A. *J. Catal.* **2017**, *346*, 154−160.
(32) Hunter, R.; Hutchings, G. J. *J. Chem. Soc., Chem. Commun.* **1987**, 377−379.
(33) Martinez-Espin, J. S.; Morten, M.; Janssens, T. V. W.; Svelle, S.; Beato, P.; Olsbye, U. *Catal. Sci. Technol.* **2017**, *7*, 2700−2716.
(34) Sayed, M. B. *J. Chem. Soc., Faraday Trans. 1* **1987**, *83*, 1771−1778.
(35) McCann, D. M.; Lesthaeghe, D.; Kletnieks, P. W.; Guenther, D. R.; Hayman, M. J.; Van Speybroeck, V.; Waroquier, M.; Haw, J. F. *Angew. Chem.* **2008**, *120*, 5257−5260.
(36) Zhang, M.; Xu, S.; Li, J.; Wei, Y.; Gong, Y.; Chu, Y.; Zheng, A.; Wang, J.; Zhang, W.; Wu, X.; Deng, F.; Liu, Z. *J. Catal.* **2016**, *335*, 47−57.
(37) Tuma, C.; Sauer, J. *Angew. Chem., Int. Ed.* **2005**, *44*, 4769−4771.
(38) Cnudde, P.; De Wispelaere, K.; Van der Mynsbrugge, J.; Waroquier, M.; Van Speybroeck, V. *J. Catal.* **2017**, *345*, 53−69.
(39) Bleken, B. T. L.; Wragg, D. S.; Arstad, B.; Gunnæs, A. E.; Mouzon, J.; Helveg, S.; Lundegaard, L. F.; Beato, P.; Bordiga, S.; Olsbye, U.; Svelle, S.; Lillerud, K. P. *Top. Catal.* **2013**, *56*, 558−566.
(40) Choi, M.; Na, K.; Kim, J.; Sakamoto, Y.; Terasaki, O.; Ryoo, R. *Nature* **2009**, *461*, 246−249.
(41) Kresse, G.; Joubert, D. *Phys. Rev. B: Condens. Matter Mater. Phys.* **1999**, *59*, 1758−1775.
(42) Kresse, G.; Furthmüller, J. *Phys. Rev. B: Condens. Matter Mater. Phys.* **1996**, *54*, 11169−11186.
(43) Kresse, G.; Furthmüller, J. *Comput. Mater. Sci.* **1996**, *6*, 15−50.
(44) Kresse, G.; Hafner, J. *Phys. Rev. B: Condens. Matter Mater. Phys.* **1994**, *49*, 14251−14269.
(45) Kresse, G.; Hafner, J. *Phys. Rev. B: Condens. Matter Mater. Phys.* **1993**, *47*, 558−561.
(46) Hajek, J.; Van Der Mynsbrugge, J.; De Wispelaere, K.; Cnudde, P.; Vanduyfhuys, L.; Waroquier, M.; Van Speybroeck, V. *J. Catal.* **2016**, *340*, 227−235.
(47) Van Der Mynsbrugge, J.; Moors, S. L. C.; De Wispelaere, K.; Van Speybroeck, V. *ChemCatChem* **2014**, *6*, 1906−1918.
(48) Ghysels, A.; Verstraelen, T.; Hemelsoet, K.; Waroquier, M.; Van Speybroeck, V. *J. Chem. Inf. Model.* **2010**, *50*, 1736−1750.
(49) De Moor, B. A.; Reyniers, M. F.; Marin, G. B. *Phys. Chem. Chem. Phys.* **2009**, *11*, 2939−2958.
(50) Brogaard, R. Y.; Henry, R.; Schuurman, Y.; Medford, A. J.; Moses, P. G.; Beato, P.; Svelle, S.; Nørskov, J. K.; Olsbye, U. *J. Catal.* **2014**, *314*, 159−169.
(51) Vandevondele, J.; Krack, M.; Mohamed, F.; Parrinello, M.; Chassaing, T.; Hutter, J. *Comput. Phys. Commun.* **2005**, *167*, 103−128.
(52) Hutter, J.; Iannuzzi, M.; Schiffmann, F.; Vandevondele, J. *Wiley Interdisciplinary Reviews: Computational Molecular Science* **2014**, *4*, 15−25.
(53) Goedecker, S.; Teter, M.; Hutter, J. *Phys. Rev. B: Condens. Matter Mater. Phys.* **1996**, *54*, 1703−1710.
(54) Martyna, G. J.; Tobias, D. J.; Klein, M. L. *J. Chem. Phys.* **1994**, *101*, 4177−4189.
(55) Frenkel, D.; Smit, B. In *Understanding Molecular Simulation*, 2nd ed.; Academic Press: San Diego, 2002.
(56) Yamazaki, H.; Shima, H.; Imai, H.; Yokoi, T.; Tatsumi, T.; Kondo, J. N. *J. Phys. Chem. C* **2012**, *116*, 24091−24097.
(57) Bjørgen, M.; Joensen, F.; Lillerud, K. P.; Olsbye, U.; Svelle, S. *Catal. Today* **2009**, *142*, 90−97.
(58) Wei, Z.; Chen, Y.; Li, J.; Guo, W.; Wang, S.; Dong, M.; Qin, Z.; Wang, J.; Jiao, H.; Fan, W. *J. Phys. Chem. C* **2016**, *120*, 6075−6087.
(59) Wu, X.; Xu, S.; Zhang, W.; Huang, J.; Li, J.; Yu, B.; Wei, Y.; Liu, Z. *Angew. Chem., Int. Ed.* **2017**, *56*, 9039−9043.
(60) Chang, C. D.; Lang, W. H.; Bell, W. K. *Catalysis of Organic Reactions*; Moser, W. R., Ed.; Dekker: 1981; p 73.
(61) Ai, M. *J. Catal.* **1987**, *106*, 280−286.
(62) Ivanova, I.; Sushkevich, V. L.; Kolyagin, Y. G.; Ordomsky, V. V. *Angew. Chem., Int. Ed.* **2013**, *52*, 12961−12964.
(63) Haw, J. F.; Nicholas, J. B.; Song, W.; Deng, F.; Wang, Z.; Xu, T.; Heneghan, C. S. *J. Am. Chem. Soc.* **2000**, *122*, 4763−4775.
(64) Dai, W.; Wang, C.; Dyballa, M.; Wu, G.; Guan, N.; Li, L.; Xie, Z.; Hunger, M. *ACS Catal.* **2015**, *5*, 317−326.
(65) Van Speybroeck, V.; Van der Mynsbrugge, J.; Vandichel, M.; Hemelsoet, K.; Lesthaeghe, D.; Ghysels, A.; Marin, G. B.; Waroquier, M. *J. Am. Chem. Soc.* **2011**, *133*, 888−899.
(66) Van Speybroeck, V.; De Wispelaere, K.; Van Der Mynsbrugge, J.; Vandichel, M.; Hemelsoet, K.; Waroquier, M. *Chem. Soc. Rev.* **2014**, *43*, 7326−7357.
(67) De Wispelaere, K.; Bailleul, S.; Van Speybroeck, V. *Catal. Sci. Technol.* **2016**, *6*, 2686−2705.
(68) Wei, Z. H.; Chen, Y. Y.; Li, J. F.; Guo, W. P.; Wang, S.; Dong, M.; Qin, Z. F.; Wang, J. G.; Jiao, H. J.; Fan, W. B. *J. Phys. Chem. C* **2016**, *120*, 6075−6087.
(69) Lesthaeghe, D.; Van Speybroeck, V.; Marin, G. B.; Waroquier, M. *Angew. Chem., Int. Ed.* **2006**, *45*, 1714−1719.